Electromagnetically Induced Transparency and Absorption in Directly Coupled Whispering-Gallery Mode Microcavities

Xu Huang, Tie-Jun Wang, *Member, IEEE*, and Chuan Wang, *Member, IEEE*

***Abstract*—Optical interference and the related effects are key elements which could exhibit the properties of both classical and quantum optical systems. Usually, the interference between different optical paths may produce intriguing effects, such as the electromagnetically induced transparent (EIT) and so on. In this work, we study the interference effects in directly coupled whispering-gallery mode (WGM) micro-resonators, in which the emergence of EIT and electromagnetically induced absorption (EIA) could be observed. We find by tuning the coupling strength between the resonators, the modulation phase may control the appearance and disappearance of EIT (EIA). Furthermore, we prove the existence of fast and slow light, and propose a scheme for effective switching between them. This work provides a new strategy for obtaining slow light and quantum storage in the WGM micro-resonators.**

***Index Terms*—Electromagnetically induced transparency, whispering-gallery mode, directly coupled.**

I. Introduction

OPTICAL interference is a typical effect in both classical and quantum optics. And it has been widely demonstrated in nanophotonic devices, such as in the plasmonic devices and optical microcavities. Recently, optical microcavities have been extensively studied due to their advantages in isolating modes that meet specific conditions from the continuous mode by resonance and confining them to a small volume on the order of micrometers [1], [2]. Usually, there are several typical configurations of optical microcavities, such as the Fabry-Perot microcavities [3], whispering-gallery mode (WGM) optical microcavities [4]–[10], distributed feedback (DFB) microcavities [11], and photonic crystal microcavities [12].

Specifically, in the WGM optical microcavities, the resonant light field is restricted by the total internal reflection and circulates around the curved inner boundary of the optical microcavities. This special architecture can greatly enhance the light-matter interactions due to the high quality factor and small mode volume [13]–[19]. The unique advantages of WGM optical microcavities have been proven in several field both theoretically and experimentally, such as the parity-time-symmetry optics [20]–[26], ultralow threshold laser [27]–[30], nonlinear optics [13], [31]–[34], optical quantum information processing [35], [36], cavity quantum electrodynamics [17], [37], [38], and second or high-order harmonic generation [39], [40].

Moreover, the optical evanescent field in the WGM microcavities exhibits a very wide distribution, which can well couple modes out of the cavity or into the cavity. And any changes in or near the periphery of the cavity could be detected. These special features made it various applications in cavity optomechanics [41]–[49], high-precision sensing [50]–[58], phonon lasers [23], [59], [60], and biosensing [61]–[66].

In quantum optics, the electromagnetically induced transparency (EIT) and electromagnetically induced absorption (EIA) is a typical interference effect which could be illustrated by the interference between different levels transition in atomic structures [67]–[69]. EIT relies on destructive interference, which leads to the absorption suppression. EIA is due to coherent interaction with optical radiation. EIT resonance peak provides high dispersion and very low absorption of light, EIA also has high dispersion, so they can be used for low-light level nonlinear optics. For example, EIT and related effects in atomic ensemble systems [67], [70]–[73], optomechanical [46], [74], [75], microwave field [76], plasmonic [77], coupled microcavities [78]–[81], directly or indirectly coupled microrings on a chip [82]–[84]. Recently, the applications of WGM microcavities in EIT have gradually attracted attentions, the EIT effect has been observed in coupled WGM microcavities [85], [86]. The coupled resonator induced transparency and absorption caused by the interference between the WGM microcavities is also demonstrated [87]. And the transparency and absorption of chiral light state modulation at anomalous points in an indirect coupled resonator system is also discussed [88]. From these results, EIT or EIA can be obtained by tuning the coupling strength and phase control of the resonator, which provides a new method for obtaining slow light [89], ground state cooling [90], second-harmonic generation [91] and quantum storage [92].

Manuscript received December 17, 2021; revised February 8, 2022; accepted February 11, 2022. Date of publication February 14, 2022; date of current version February 24, 2022. This work was supported in part by the National Natural Science Foundation of China under Grants 62131002 and 62071064, in part by the Fundamental Research Funds for the Central Universities of China under Grant 2019XD-A02, in part by the Fundamental Research Funds for the Central Universities, and in part by the Fund of State Key Laboratory of Information Photonics and Optical Communications, Beijing University of Posts and Telecommunications, China. *(Corresponding author: Tie-Jun Wang.)*

Xu Huang and Tie-Jun Wang are with the School of Science, Beijing University of Posts and Telecommunications, Beijing 100876, China (e-mail: huangx@bupt.edu.cn; wangtiejun@bupt.edu.cn).

Chuan Wang is with the School of Artificial Intelligence, Beijing Normal University, Beijing 100875, China (e-mail: wangchuan@bnu.edu.cn).

Digital Object Identifier 10.1109/JPHOT.2022.3151506

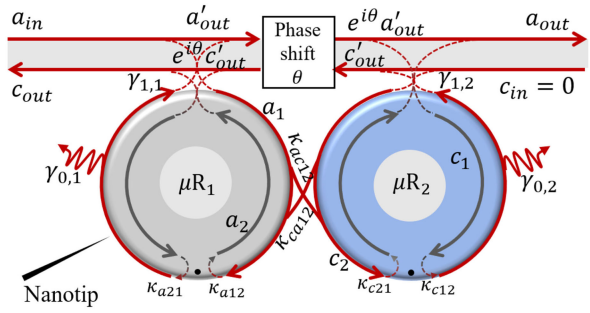

Fig. 1. System model diagram of two directly coupled WGM microcavities. The two WGM microcavities are directly coupled, and are respectively coupled to the optical fiber through the evanescent field. There are inherent disturbances in the two resonators to couple the CW mode and the CCW mode. A nanotip is introduced on the resonator μR_1. (b) The resonators μR_1 and μR_2 are coupled to the fiber cone with coupling strengths $\gamma_{1,1}$ and $\gamma_{1,2}$, respectively. They all support CW and CCW modes ($a_{1,2}$ and $c_{1,2}$) with inherent losses ($\gamma_{0,1}$ and $\gamma_{0,2}$).κ_{a12}, κ_{a21}, and κ_{c12}, κ_{c21} are the coupling strengths of CW and CCW modes in resonators μR_1 and μR_2, respectively.κ_{ac12}, κ_{ca12} are the coupling strength of CW and CCW modes between the two resonators.

In this work, we mainly study the destructive interference induced by nanoscatters in the micro-resonators. The resonant system is composed of two directly coupled WGM optical microcavities which are simultaneously coupled to the same fiber tapered waveguide. Here, the clockwise (CW) mode and the counterclockwise (CCW) mode are coupled through inherent perturbation. After the introduction of nanoscatters, the symmetry of the CW mode and CCW mode of the system would be destroyed. Therefore, the destructive interference can be used to induce the transparency window on the spectrum. Moreover, EIT or EIA can be achieved by modulating the coupling strength between the resonators, and the mutual conversion between EIT and EIA can also be realized by changing the coupling strength. It is worth noting that the appearance of EIT and EIA is required under a certain phase condition, so we can also selectively induce transparency or absorption by modulating the phase. We believe this work may provide a new strategy for the fast or slow light generation and switching in the nanophotonic system.

II. Theoretical Model

The principle of the system is shown in Fig. 1, in which two WGM microcavities are simultaneously coupled to the fiber tapered waveguide and also directly coupled to each other.Compared with the previously indirectly coupled microcavities induced EIT [85], the directly coupled microcavity provides more flexibility for EIT. Here ω_a and ω_c are the resonant frequencies of the two WGM microcavities μR_1 and μR_2, respectively, and the natural damping rates are $\gamma_{0,1}$, $\gamma_{0,2}$. The WGM microcavities μR_1 is driven by a pump field with frequency ω. The amplitude of the pump field is $E=\sqrt{P/\hbar\omega}$, where P denotes the pump power. The two microcavities μR_1 and μR_2 are coupled to the waveguide with the coupling strength of $\gamma_{1,1}$ and $\gamma_{1,2}$. According to the coupled-mode theory [93],when determining the coupling strength, there are two crucial factors:the amount of overlap between modes and the phase-matching between them. As long as the field distribution of the waveguide and the microsphere is available, the coupling coefficient can be obtained by the integral formula, which is equivalent to the integral formula given in [94], [95]:

$$\gamma_{1,1}=\frac{\omega\Delta\epsilon}{4}\iiint_{V_{\mu R_1}}\vec{E}_f\cdot\vec{E}^*_{\mu R_1}\cdot e^{i\Delta\beta_1 z}\mathrm{d}v \tag{1}$$

$$\gamma_{1,2}=\frac{\omega\Delta\epsilon}{4}\iiint_{V_{\mu R_2}}\vec{E}_f\cdot\vec{E}^*_{\mu R_2}\cdot e^{i\Delta\beta_2 z}\mathrm{d}v \tag{2}$$

where $\Delta\epsilon=\epsilon_0(n_s^2-n_0^2)$ denotes the permittivity difference between the micro-resonator (the same material as the taper) and the air,n_s and n_0 are the indices of refraction of the micro-resonator and air. $\vec{E}_f$ and $\vec{E}_{\mu R_1(\mu R_2)}$are the normalized fields of the fiber and the micro-resonator, which are defined by $1/2\iint\sqrt{\varepsilon/\mu_0}|\vec{E}_{f(\mu R_1,\mu R_2)}|^2\,\mathrm{d}x\,\mathrm{d}y=1$,and $V_{\mu R_1(\mu R_2)}$ is volume of the micro-resonator $\mu R_1(\mu R_2)$.$\Delta\beta_{1(2)}=\beta_f-\beta_{\mu R_1(\mu R_2)}$ defines the difference in propagation constants of the taper and the micro-resonator.

CW mode and CCW mode are coupled to each other through the backscattering of the microcavities surface. In μR_2, we assume that the coupling strength from CW to CCW (κ_{c12}) is the same as that from CCW to CW (κ_{c21}). In the evanescent field of μR_1, the silica nanotip controlled by nano-positioners is placed as the rayleigh scatterers. The nano-positioners could adjust the relative position and effective size of the nanotips in the evanescent field of μR_1. The additional perturbation introduced into the nanometer tip leads to asymmetric backscattering, that is, the scattering-induced coupling strength from CW to CCW (κ_{a12}) is not equal to the scattering-induced coupling strength from CCW to CW (κ_{c21}).When analyzing the mode coupling between two microresonators, considering that the CW (CCW) in μR_1 is coupled into μR_2 in the CCW (CW) direction, so it is not considered that the CW (CCW) in μR_1 is coupled into the CW (CCW) in μR_2 in the same direction,and the coupling from μR_2 to μR_1 is the same.Moreover, we assume that the direct coupling resonators μR_1 and μR_2 have the same coupling strength in different directional modes.which means the coupling strength from CW mode in μR_1 to CCW mode in μR_2 (κ_{ac12}), from CCW in μR_1 to CW in μR_2 (κ_{ac21}), from CW in μR_2 to CCW in μR_1 (κ_{ca12}) and from CCW in μR_2 to CCW in μR_1 (κ_{ca21}) are all equal.According to the coupled mode theory, referring to the coupling strength of a fiber taper coupled to a micro-resonator ((1),(2)), we have obtained the coupling strength between micro-resonators:

$$\kappa_{ac12}=\frac{\omega\Delta\epsilon}{4}\iiint_{V_{\mu R_2}}\vec{E}_{\mu R_1,CW}\cdot\vec{E}^*_{\mu R_2,CCW}\cdot e^{i\Delta\beta z}\mathrm{d}v \tag{3}$$

where $\vec{E}_{\mu R_1,CW}$ and $\vec{E}_{\mu R_2,CCW}$ are the normalized fields of of CW mode in μR_1 and CCW mode in μR_2, and β is the difference in propagation constants of these two modes.Similarly, κ_{ac21}, κ_{ca12}, and κ_{ca21} can also be achieved by integrating the normalized field and the propagation constant difference of the two coupled modes.It can be seen from (3) that we can change the amount of overlap between modes to change the coupling strength.

The Hamiltonian of the system is composed of the free Hamiltonian H_0, the Hamiltonian of the internal interaction H_{II} and

the Hamiltonian of the interaction between the microresonators H_{MI}, which can be described as

$$H = H_0 + H_{II} + H_{MI}, \tag{4}$$

$$H_0 = \hbar\omega_a a_1^\dagger a_1 + \hbar\omega_a a_2^\dagger a_2 + \hbar\omega_c c_1^\dagger c_1 + \hbar\omega_c c_2^\dagger c_2, \tag{5}$$

$$H_{II} = \hbar\kappa_{a12} a_1^\dagger a_2 + \hbar\kappa_{a21} a_2^\dagger a_1 + \hbar\kappa_{c12} c_1^\dagger c_2 + \hbar\kappa_{c21} c_2^\dagger c_1, \tag{6}$$

$$H_{MI} = \hbar\kappa_{ac12} a_1^\dagger c_2 + \hbar\kappa_{ac21} a_2^\dagger c_1 + \hbar\kappa_{ca12} c_1^\dagger a_2 + \hbar\kappa_{ca21} c_2^\dagger a_1, \tag{7}$$

where a_1 and a_2 are the CW and CCW modes of $\mu\mathrm{R}_1$, and c_1 and c_2 denote the CW and CCW modes of $\mu\mathrm{R}_2$. By adding the dissipative term, the Heisenberg-Langevin dynamic equations of the system could be expressed as

$$\frac{da_1}{dt} = -i\omega_a a_1 - \frac{\gamma_{0,1}+\gamma_{1,1}}{2} a_1 - i\kappa_{a21} a_2 - \sqrt{\gamma_{1,1}} a_{in} - i\kappa_{ca21} c_2 + \Gamma_{a1}(t), \tag{8}$$

$$\frac{da_2}{dt} = -i\omega_a a_2 - \frac{\gamma_{0,1}+\gamma_{1,1}}{2} a_2 - i\kappa_{a12} a_1 - e^{i\theta}\sqrt{\gamma_{1,1}\gamma_{1,2}} c_2 - i\kappa_{ca12} c_1 + \Gamma_{a2}(t), \tag{9}$$

$$\frac{dc_1}{dt} = -i\omega_c c_1 - \frac{\gamma_{0,2}+\gamma_{1,2}}{2} c_1 - i\kappa_{c21} c_2 - \sqrt{\gamma_{1,2}} e^{i\theta}\left(a_{in} + \sqrt{\gamma_{1,1}} a_1\right), - i\kappa_{ac21} a_2 + \Gamma_{c1}(t); \tag{10}$$

$$\frac{dc_2}{dt} = -i\omega_c c_2 - \frac{\gamma_{0,2}+\gamma_{1,2}}{2} c_2 - i\kappa_{c12} c_1 - i\kappa_{ac12} a_1 + +\Gamma_{c2}(t). \tag{11}$$

In the rotating coordinate system with pump field ω as the frequency, we set detuning $\Delta_1 = \omega - \omega_a$, $\Delta_2 = \omega - \omega_c$, and total dissipation $\gamma_1 = (\gamma_{0,1} + \gamma_{1,1})/2, \gamma_2 = (\gamma_{0,2} + \gamma_{1,2})/2$. $\Gamma_{a1}(t)$, $\Gamma_{a2}(t)$, $\Gamma_{c1}(t)$ and $\Gamma_{c2}(t)$ represent fluctuation operators corresponding to the modes a_1, a_2, c_1, and c_2.Using the semiclassical and mean-field approximations,the steady state solution could be solved as:

$$a_1 = (\gamma_2 + i\Delta_2)\frac{\sqrt{\gamma_{1,2}} e^{i\theta}\lambda\Theta - \sqrt{\gamma_{1,1}}\lambda\xi}{\Xi\xi - \Theta\mu} a_{in}; \tag{12}$$

$$c_1 = -\frac{\mu a_1 + (\gamma_2 + i\Delta_2)\sqrt{\gamma_{1,2}} e^{i\theta}\lambda a_{in}}{\xi}; \tag{13}$$

$$a_2 = \frac{\alpha a_1 + \beta c_1}{\lambda}; \tag{14}$$

$$c_2 = -\frac{i}{\gamma_2 + i\Delta_2}\left(\kappa_{c12} c_1 + \kappa_{ac12} a_1 + \kappa_{ac22} a_2\right). \tag{15}$$

Here the related parameters in the above could be expressed as:

$$\alpha = i(\gamma_2 + i\Delta_2)\kappa_{a12} - ie^{i\theta}\sqrt{\gamma_{1,1}\gamma_{1,2}}\kappa_{ac12},$$

$$\beta = i(\gamma_2 + i\Delta_2)\kappa_{ca12} - ie^{i\theta}\sqrt{\gamma_{1,1}\gamma_{1,2}}\kappa_{c12},$$

$$\lambda = -(\gamma_1 + i\Delta_1)(\gamma_2 + i\Delta_2),$$

$$\mu = \left(\kappa_{c12}\kappa_{ac12} + (\gamma_2 + i\Delta_2)\sqrt{\gamma_{1,1}\gamma_{1,2}} e^{i\theta}\right)\lambda + i(\gamma_2 + i\Delta_2)\kappa_{ac21}\alpha,$$

$$\xi = \left[(\gamma_2 + i\Delta_2)^2 + \kappa_{c21}\kappa_{c12}\right]\lambda + i(\gamma_2 + i\Delta_2)\kappa_{ac21}\beta;$$

$$\Xi = (\gamma_1 + i\Delta_1)(\gamma_2 + i\Delta_2)\lambda + i(\gamma_2 + i\Delta_2)\kappa_{a21}\alpha + \kappa_{ca21}\kappa_{ac12}\lambda,$$

$$\Theta = i(\gamma_2 + i\Delta_2)\kappa_{a21}\beta + \kappa_{ca21}\kappa_{c12}\lambda.$$

The angle θ is the phase shift accumulated when light propagates in the fibre between the resonators.Based on the well-known input-output relation [96], the output field is given by:

$$a_{\text{out}} = \sqrt{\gamma_{1,2}} c_1 + e^{i\theta}\left(\sqrt{\gamma_{1,1}} a_1 + a_{in}\right), \tag{16}$$

$$c_{\text{out}} = \sqrt{\gamma_{1,1}} a_2 + e^{i\theta}\sqrt{\gamma_{1,2}} c_2. \tag{17}$$

And the transmission spectrum could be solved as:

$$\mathrm{T} = |t_p|^2 = \left|\frac{a_{\text{out}}}{a_{\text{in}}}\right|^2 = \left|(\gamma_2 + i\Delta_2)\left(e^{i\theta}\sqrt{\gamma_{1,1}} - \frac{\sqrt{\gamma_{1,2}}\mu}{\xi}\right)\frac{\sqrt{\gamma_{1,2}} e^{i\theta}\lambda\Theta - \sqrt{\gamma_{1,1}}\lambda}{\Xi\xi - \Theta\mu} + \left(e^{i\theta} - \frac{(\gamma_2 + i\Delta_2)\gamma_{1,2} e^{i\theta}\lambda}{\xi}\right)\right|^2. \tag{18}$$

And the associated transmission group delay caused by the rapid phase dispersion is given by

$$\tau = \frac{d\arg(t_p)}{d\Delta}, \tag{19}$$

where $\arg(t_p)$ takes the argument of the complex number t_p.

III. Results and Discussions

Considering the performance of the nanoscatters, the perturbation would be induced on the transmission spectrum. And after the direct coupling of the two microresonators, the effects of weak coupling(strong coupling) on the transmission spectrum are also required to be considered. Moreover, we also analyze the influence of phase θ modulation on the transmission spectrum.

It is obvious that the interaction of nanotips in the uncoupled microcavities makes the scattering from a_1 to a_2 is $\kappa_{a12} = 0$. In the case of $\gamma_{1,1} \gg \gamma_{0,1}$, $\gamma_{1,2} \approx \gamma_{0,2}$, the simplification of (18) can be obtained as:

$$T = \left|\frac{\gamma_1\kappa_{b21}\kappa_{b12}}{2\gamma_2\kappa_{a21}\kappa_{b12}e^{2i\theta} + \gamma_1\gamma_2^2 + \gamma_1\kappa_{b21}\kappa_{b12}}\right|^2 \tag{20}$$

According to the above results, we refer to the parameters in the previous report [88]. Correspondingly, the results of simulating on the transmission spectrum is shown in Fig. 2(a). Here, we consider the frequency detuning fulfills the relation $\Delta_1 = \Delta_2 = \Delta = 0$. In Fig. 2(a), when the nanoscatter is not introduced (see the blue solid line), it can be clearly seen that the transmission rate T is relatively low. When the phase is around

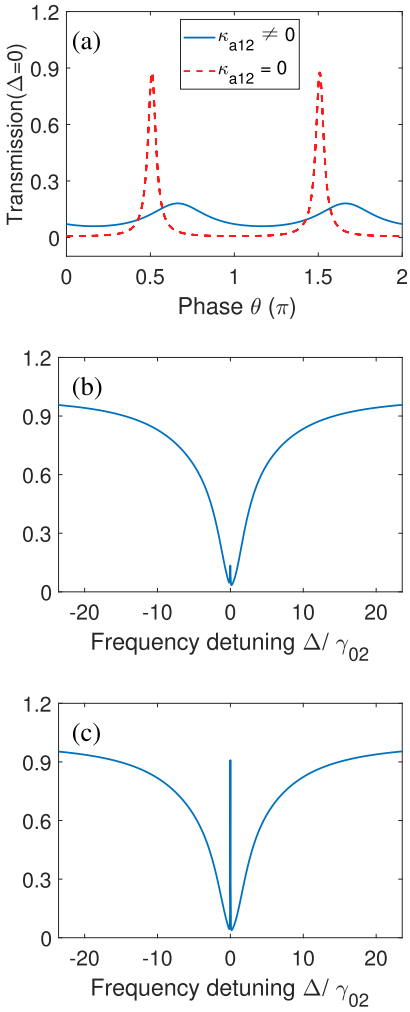

Fig. 2. The transmission T of the system before and after adding the nanotip when the system is uncoupled. (a) Transmission as a function of modulation phase θ, we estimated the relevant parameters as $\lambda = 1447.6\,\mathrm{nm}$, $\gamma_{0,1} = 14.61\,\mathrm{MHz}$, $\gamma_{1,1} = 148.12\,\mathrm{MHz}$, $\gamma_{0,2} = 5.33\,\mathrm{GHz}$, $\gamma_{1,2} = 3.6\,\mathrm{GHz}$, $\kappa_{a12} = 0$ (the red dashed line) and $\kappa_{a12} = (11.79 + 74.31\mathrm{i})\mathrm{MHz}$ (the blue solid line), $\kappa_{a21} = (11.79 + 74.31\mathrm{i})\mathrm{MHz}$, $\kappa_{c12} = \kappa_{c21} = (1.30 \times 10^2 - 2.60 \times 10^3\mathrm{i})\mathrm{MHz}$. (b), (c) The transmission spectrum of the system before and after the nanotip interaction at $\theta = 0.517\pi$.

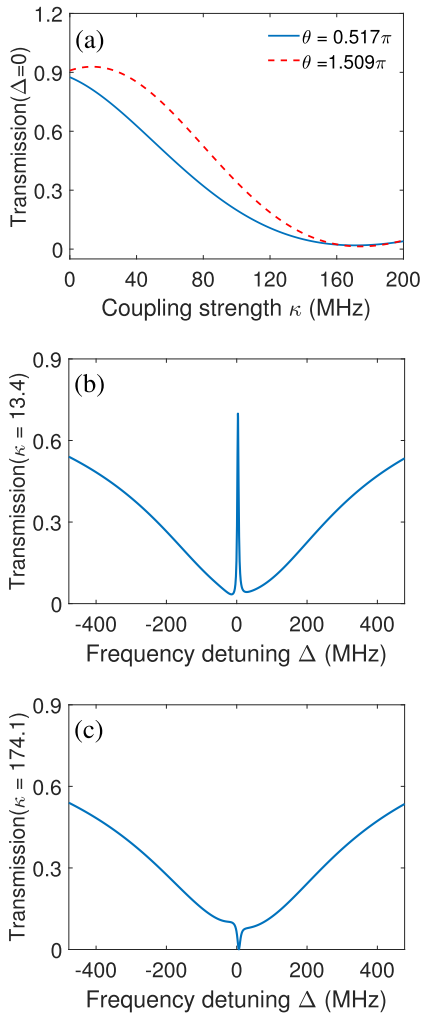

Fig. 3. (a) After two microcavities are directly coupled, transmission T as a function of the coupling strength κ between two resonators when the phase is $\theta = 0.517\pi$(the blue solid line) and $\theta = 1.509\pi$(the red dashed line). Here, we consider $\Delta = 0$. (b) Transmission T as a function of the detuning Δ, and we take the coupling strength $\kappa = 13.4\,\mathrm{MHz}$. (c) T versus κ when the coupling strength $\kappa = 174.1\,\mathrm{MHz}$.

$\theta = 0.65\pi$, the transmission T is only about 0.13, and when the nanoscatter is introduced (see the red dashed line), we can see that the transmission rate has increased significantly. When the phase is around $\theta = 0.52\pi$, the transmission approaches about 0.91, and it can be concluded that the transmission has been improved several times after introduction of the nanoscatter. This is because the nanoscatter is an external perturbation of the system, so that the CCW mode (a_1) in the $\mu\mathrm{R}_1$ cavity cannot be transmitted to the $\mu\mathrm{R}_2$ cavity. Meanwhile, this caused the asymmetric distribution of field in the system. And according to Fig. 2(a), we can see that the transmission T changes periodically with the increment of θ, so we can modulate the transmission rate T by tuning the phase θ.We noticed that there is a phase shift in Fig. 2(a). This is because the nanotip introduces an extra phase, which causes the resonance phase of the system to shift. Fig. 2(b) and 2(c) show the change of the transmission T with the detuning Δ before and after adding the nanotip, when the detuning is $\Delta_1 = \Delta_2 = \Delta$. It can be analyzed from (20) that when the relation $2\kappa_{a21}\kappa_{c12}e^{2i\theta} = -\gamma_1\gamma_2$ is satisfied, the maximal transmission rate of the system can approach unity. Meanwhile, it can be seen from Fig. 2(c) that it is consistent with the theoretical prediction, which proves that the efficiency of the EIT window can be improved by the nanoscatters.

Here in the following, we consider the directly coupled resonators, the coupling strength between two resonators is the same as $\kappa_{ac12} = \kappa_{ac21} = \kappa_{ca12} = \kappa_{ca21} = \kappa$. In Fig. 3(a), it can be seen that when $\theta = 0.517\pi$ (the blue solid line), the transmission T is directly decreased. When the coupling strength between the two resonators reaches $\kappa = 171.2\,\mathrm{MHz}$, there is a minimal value of 0.019 could be obtained in the spectrum which appears the induced absorption. Further by increasing $\theta = 1.509\pi$ (the red dashed line), the transmission spectrum rises first. When the coupling strength between the two resonators is $\kappa = 13.4\,\mathrm{MHz}$, the maximal value of transmission

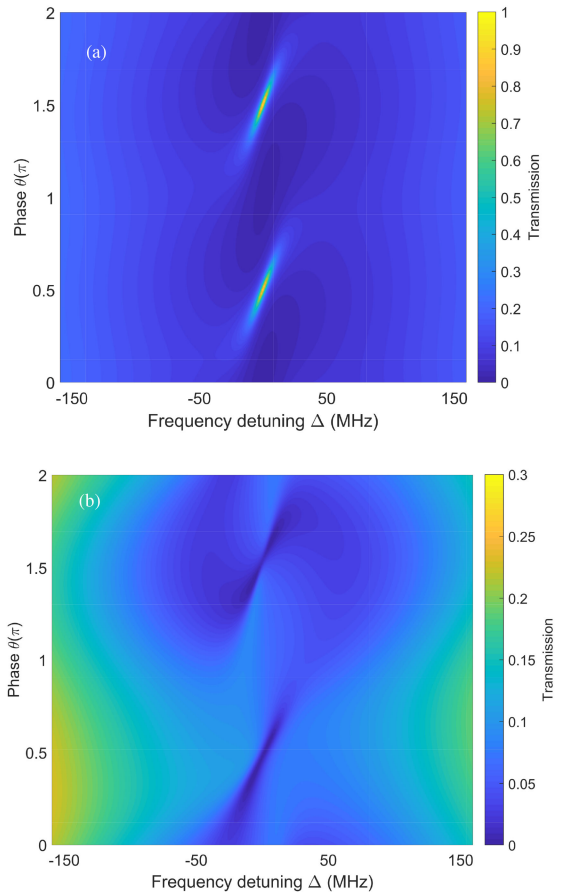

Fig. 4. (a) Transmission spectrum at the coupling strength between two resonators is $\kappa = 13.4\,\mathrm{MHz}$ with the variation of the detuning Δ and the change in phase θ under the ideal conditions. (b) Transmission spectrum versus the detuning amount Δ and the phase θ when the coupling strength is $\kappa = 174.1\,\mathrm{MHz}$.

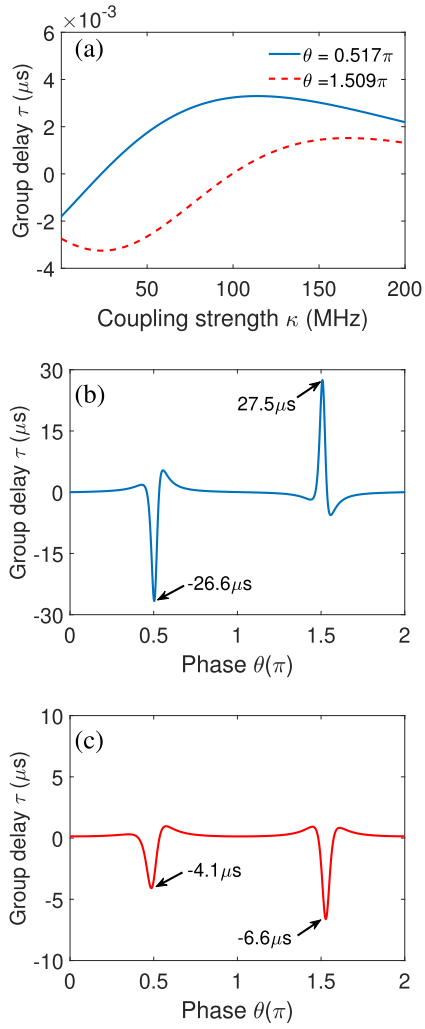

Fig. 5. (a) In the case of a transmission window of $\Delta = 0$, optical group delay τ as a function of the coupling strength at phase $\theta = 0.517\pi$(the blue solid line) and $\theta = 1.509\pi$(the red dashed line) respectively. (b), (c) Optical group delay τ as a function of the phase at coupling strength $\kappa = 23.7\,\mathrm{MHz}$ and $\kappa = 167.8\,\mathrm{MHz}$, respectively.

rate is approaching 0.929 (see Fig. 3(b)). Then, the transmission spectrum decreases as the coupling strength between the two resonators increases. We get the minimal value of 0.014 in the transmission spectrum, when the coupling strength increases to $\kappa = 174.1\,\mathrm{MHz}$, accompanied with the phenomenon of induced absorption will appear(see Fig. 3(c)). Moreover, we can obtain the ideal transmission spectrum by adjusting the coupling strength at different phases.

Now, we analyze the system transmission T as a function of the detuning Δ and the phase θ, when the coupling strength between the two resonators is $\kappa = 13.4\,\mathrm{MHz}$ (see Fig. 4(a)), we can see the maximal value at $\theta = 0.517\,\pi$ and $\theta = 1.519\pi$, so the system would reach a state of induced transparency by modulating the phase. Also the emergence of EIT can be achieved by tuning the modulating phase θ. Similarly, we also analyze when the coupling strength between the two resonators is $\kappa = 174.1\,\mathrm{MHz}$ (see Fig. 4(b)), the influence of detuning Δ and phase θ on the transmission of the system, we can see that there is induced absorption at $\theta = 0.517\pi$ and $\theta = 1.519\pi$. Furthermore, we also can adjust the coupling strength κ between the microcavities to make the conversion of the system transition spectrum from the state in Fig. 4(a) to the state in Fig. 4(b), and realize the state transition between induced transparency and induced absorption. Compared with the classical coupled microcavities [79], [80] to obtain EIT by changing the coupling strength, we can also adjust the phase accumulation θ to generate EIT.

In general,the important characteristics of EIT and EIA are narrow spectral width and steep dispersion. The characteristic of steep dispersion helps to control the group speed of light pulses. By adjusting the normal dispersion of EIT and the abnormal dispersion of EIA, the group speed of light pulses can be slowed down or speed up respectively. The optical group delay can be created due to the fact that the dispersion curve varies drastically with the frequency within the EIT window [89], which is useful in optical information storage without absorption. Correspondingly, the information speed of fast light under EIA is attractive [97], [98]. In this case, the slow-light effect emerges in the transmission window of $\Delta = 0$ (see Fig. 5(a)). When the phase $\theta = 0.517\pi$, the group delay first gradually increases, approaches the maximal value at the coupling strength

$\kappa = 114.6\,\mathrm{MHz}$, and then gradually decreases (see the solid blue line in Fig. 5(a)). When the phase $\theta = 1.509\pi$, the group delay first decreases gradually, then it reaches a minimal value when the coupling strength $\kappa = 23.7\,\mathrm{MHz}$. After that, the group delay gradually increases, approaches a minimal value when the coupling strength $\kappa = 167.8\,\mathrm{MHz}$ (see the red dashed line in Fig. 5(a)).

In the case of a transmission window with $\Delta = 0$, we also plot the optical group delay τ as a function of the modulation phase θ at the coupling strength $\kappa = 23.7\,\mathrm{MHz}$ (see Fig. 5(b)) and the coupling strength $\kappa = 167.8\,\mathrm{MHz}$ (see Fig. 5(c)). The group delay time significantly decreases at $\theta = 0.503\,\pi$, the delay time of the light can even reach $-26.6\,\mu$s, and the group delay time significantly increases at $\theta = 1.508\,\pi$. Finally, the group delay of the light can even approach $27.5\,\mu$s (see Fig. 5(b)). Therefore, we can switch between fast and slow light at the coupling strength $\kappa = 23.7\,\mathrm{MHz}$ by tuning the modulation phase θ. Meanwhile, the group delay time significantly decreases near $\theta = 0.482\,\pi$ and $\theta = 1.528\,\pi$, the delay time of the light can even reach $-4.1\,\mu$s and $-6.6\,\mu$s, respectively(see Fig. 5(c)). It is worth mentioning that near the phase $\theta = 1.515\pi$, when the coupling strength is $\kappa = 23.7\,\mathrm{MHz}$ and $\kappa = 167.8\,\mathrm{MHz}$, the group delay is with the opposite sign, which means that the slow-to-fast and fast-to-slow light effects can emerge by changing the coupling strength.Compared with the slow light in the classic EIT [99], [100], the group delay of our slow light has improved by nearly an order of magnitude, and we have also studied the fast light effects in the system. These results can lead to achieve the ultraslowing or ultra-fast signals, which can be used in optical storage and quantum communication.

Different from the previous studies of obtaining EIT and EIA in a coupled optical microcavity [87], [101], there is direct coupling of the fiber taper to the second microcavity in our system, which enables the modes in the two microcavities to be coupled through the fiber. Therefore, we can not only obtain EIT and EIA by adjusting the coupling strength, but also control the appearance of EIT and EIA by adjusting the accumulated phase in the fiber.We also give the specific effects of the coupling strength between the two microcavities and the cumulative phase on the EIT and EIA. What's more, we analyze the fast and slow light conditions that exist under this model, which are not present in previous work.This makes our work potentially applicable in amplitude-based high-sensitivity sensing and quantum information processing.

IV. Summary

In summary, based on the directly coupled waveguide and microcavities system, we study the EIT and EIA effects in the proposed system. The inherent perturbation of the surface of the cavity induces the coupling between the CW mode and the CCW mode. We obtain the analytical expression of the transmission spectrum by solving the dynamic equations of the system. First, the efficiency of the EIT is increased by introducing nanoprobes. Secondly, the influence of different coupling intensities on the transmission spectrum is studied. The results show that strong EIT can be achieved under the weak coupling, but EIA occurs under strong coupling strength. Therefore, we can achieve the conversion between EIT and EIA by tuning the coupling strength.The transmission spectra under different phases is also discussed, which can be selected to obtain EIT (EIA) by modulating the phases. Finally, the conditions for the existence of fast or slow light are proved in the directly coupled WGM microcavities, and a conversion strategy that can realize fast light to slow light or slow light to fast light is given. We believe our work has enriched the acquisition methods and mutual switching of EIT and EIA in the nanophotonic devices, and provide a novel way for the acquisition of slow light and quantum storage.

References

[1] R. K. Chang and A. J. Campillo, *Optical Processes in Microcavities*, vol. 3. Singapore: World Scientific, 1996.

[2] T. J. Wang, C. Cao, and C. Wang, "On the developments and applications of optical microcavities: An overview," *Sci. China Inf. Sci.*, vol. 56, no. 12, pp. 1–15, 2013.

[3] J. M. Vaughan, *The Fabry-Perot interferometer: History, Theory, Practice and Applications*, Bristol, U.K.: Adam Hilger, 1989.

[4] S. L. McCall, A. F. J. Levi, R. E. Slusher, S. J. Pearton, and R. A. Logan, "Whispering-gallery mode microdisk lasers," *Appl. Phys. Lett.*, vol. 60, no. 3, pp. 289–291, 1992.

[5] M. Cai, O. Painter, and K. J. Vahala, "Observation of critical coupling in a fiber taper to a silica-microsphere whispering-gallery mode system," *Phys. Rev. Lett.*, vol. 85, no. 1, pp. 74–77, 2000.

[6] K. J. Vahala, "Optical microcavities," *Nature*, vol. 424, no. 6950, pp. 839–846, 2003.

[7] A. Chiasera *et al.*, "Spherical whispering-gallery-mode microresonators," *Laser Photon. Rev.*, vol. 4, no. 3, pp. 457–482, 2010.

[8] L. He, Ş. K. Özdemir, and L. Yang, "Whispering gallery microcavity lasers," *Laser Photon. Rev.*, vol. 7, no. 1, pp. 60–82, 2013.

[9] S. Yang, Y. Wang, and H. Sun, "Advances and prospects for whispering gallery mode microcavities," *Adv. Opt. Mater.*, vol. 3, no. 9, pp. 1136–1162, 2015.

[10] X. F. Liu, T. J. Wang, and C. Wang, "Optothermal control of gains in erbium-doped whispering-gallery microresonators," *Opt. Lett.*, vol. 43, no. 2, pp. 326–329, 2018.

[11] T. Fujita, Y. Sato, T. Kuitani, and T. Ishihara, "Tunable polariton absorption of distributed feedback microcavities at room temperature," *Phys. Rev. B*, vol. 57, no. 19, 1998, Art. no. 12428.

[12] J. Vučković, M. Lončar, H. Mabuchi, and A. Scherer, "Design of photonic crystal microcavities for cavity QED," *Phys. Rev. E*, vol. 65, Dec. 2001, Art. no. 016608.

[13] V. B. Braginsky, M. L. Gorodetsky, and V. S. Ilchenko, "Quality-factor and nonlinear properties of optical whispering-gallery modes," *Phys. Lett. A*, vol. 137, no. 7-8, pp. 393–397, 1989.

[14] L. Collot, V. Lefèvre-Seguin, M. Brune, J. Raimond, and S. Haroche, "Very high-Q whispering-gallery mode resonances observed on fused silica microspheres," *EPL (Europhysics Lett.)*, vol. 23, no. 5, pp. 327–334, 1993.

[15] T. J. Kippenberg, S. M. Spillane, and K. J. Vahala, "Demonstration of ultra-high-Q small mode volume toroid microcavities on a chip," *Appl. Phys. Lett.*, vol. 85, no. 25, pp. 6113–6115, 2004.

[16] M. L. Povinelli *et al.*, "High-Q enhancement of attractive and repulsive optical forces between coupled whispering-gallery-mode resonators," *Opt. Exp.*, vol. 13, no. 20, pp. 8286–8295, 2005.

[17] S. M. Spillane, T. J. Kippenberg, K. J. Vahala, K. W. Goh, E. Wilcut, and H. J. Kimble, "Ultrahigh-Q toroidal microresonators for cavity quantum electrodynamics," *Phys. Rev. A*, vol. 71, no. 1, 2005, Art. no. 013817.

[18] A. B. Matsko and V. S. Ilchenko, "Optical resonators with whispering-gallery modes-part I: Basics," *IEEE J. Sel. Top. Quantum Electron.*, vol. 12, no. 1, pp. 3–14, Jan./Feb. 2006.

[19] Q. Zhang, R. Su, X. Liu, J. Xing, T. C. Sum, and Q. Xiong, "High-quality whispering-gallery-mode lasing from cesium lead halide perovskite nanoplatelets," *Adv. Funct. Mater.*, vol. 26, no. 34, pp. 6238–6245, 2016.

[20] B. Peng *et al.*, "Parity-time-symmetric whispering-gallery microcavities," *Nature Phys.*, vol. 10, no. 5, pp. 394–398, 2014.

[21] L. Chang *et al.*, "Parity-time symmetry and variable optical isolation in active-passive-coupled microresonators," *Nature Photon.*, vol. 8, no. 7, pp. 524–529, 2014.

[22] H. Hodaei, M.-A. Miri, M. Heinrich, D. N. Christodoulides, and M. Khajavikhan, "Parity-time-symmetric microring lasers," *Science*, vol. 346, no. 6212, pp. 975–978, 2014.

[23] H. Jing, S. K. Özdemir, X.-Y. Lü, J. Zhang, L. Yang, and F. Nori, "PT-symmetric phonon laser," *Phys. Rev. Lett.*, vol. 113, no. 5, 2014, Art. no. 053604.

[24] H. Jing *et al.*, "Optomechanically-induced transparency in parity-time-symmetric microresonators," *Sci. Rep.*, vol. 5, no. 1, pp. 1–7, 2015.

[25] Ş. K. Özdemir, S. Rotter, F. Nori, and L. Yang, "Parity-time symmetry and exceptional points in photonics," *Nature Mater.*, vol. 18, no. 8, pp. 783–798, 2019.

[26] W.-L. Xu, X.-F. Liu, Y. Sun, Y.-P. Gao, T.-J. Wang, and C. Wang, "Magnon-induced chaos in an optical PT-symmetric resonator," *Phys. Rev. E*, vol. 101, no. 1, 2020, Art. no. 012205.

[27] V. Sandoghdar, F. Treussart, J. Hare, V. Lefèvre-Seguin, J.-M. Raimond, and S. Haroche, "Very low threshold whispering-gallery-mode microsphere laser," *Phys. Rev. A*, vol. 54, no. 3, 1996, Art. no. R1777.

[28] S. M. Spillane, T. J. Kippenberg, and K. J. Vahala, "Ultralow-threshold Raman laser using a spherical dielectric microcavity," *Nature*, vol. 415, no. 6872, pp. 621–623, 2002.

[29] A. Polman, B. Min, J. Kalkman, T. J. Kippenberg, and K. J. Vahala, "Ultralow-threshold erbium-implanted toroidal microlaser on silicon," *Appl. Phys. Lett.*, vol. 84, no. 7, pp. 1037–1039, 2004.

[30] X.-F. Jiang *et al.*, "Highly unidirectional emission and ultralow-threshold lasing from on-chip ultrahigh-Q microcavities," *Adv. Mater.*, vol. 24, no. 35, pp. OP260–OP264, 2012.

[31] V. S. Ilchenko, A. A. Savchenkov, A. B. Matsko, and L. Maleki, "Nonlinear optics and crystalline whispering gallery mode cavities," *Phys. Rev. Lett.*, vol. 92, no. 4, 2004, Art. no. 043903.

[32] A. B. Matsko, A. A. Savchenkov, D. Strekalov, V. S. Ilchenko, and L. Maleki, "Review of applications of whispering-gallery mode resonators in photonics and nonlinear optics," *IPN Prog. Rep.*, vol. 42, no. 162, pp. 1–51, 2005.

[33] G. Lin, A. Coillet, and Y. K. Chembo, "Nonlinear photonics with high-Q whispering-gallery-mode resonators," *Adv. Opt. Photon.*, vol. 9, no. 4, pp. 828–890, 2017.

[34] X. Zhang *et al.*, "Symmetry-breaking-induced nonlinear optics at a microcavity surface," *Nature Photon.*, vol. 13, no. 1, pp. 21–24, 2019.

[35] C. Wang, Y. Zhang, G.-S. Jin, and R. Zhang, "Efficient entanglement purification of separate nitrogen-vacancy centers via coupling to microtoroidal resonators," *JOSA B*, vol. 29, no. 12, pp. 3349–3354, 2012.

[36] T.-J. Wang and C. Wang, "Universal hybrid three-qubit quantum gates assisted by a nitrogen-vacancy center coupled with a whispering-gallery-mode microresonator," *Phys. Rev. A*, vol. 90, no. 5, 2014, Art. no. 052310.

[37] S. M. Spillane, T. J. Kippenberg, O. J. Painter, and K. J. Vahala, "Ideality in a fiber-taper-coupled microresonator system for application to cavity quantum electrodynamics," *Phys. Rev. Lett.*, vol. 91, no. 4, 2003, Art. no. 043902.

[38] Y. Louyer, D. Meschede, and A. Rauschenbeutel, "Tunable whispering-gallery-mode resonators for cavity quantum electrodynamics," *Phys. Rev. A*, vol. 72, no. 3, 2005, Art. no. 031801.

[39] J. U. Fürst *et al.*, "Naturally phase-matched second-harmonic generation in a whispering-gallery-mode resonator," *Phys. Rev. Lett.*, vol. 104, no. 15, 2010, Art. no. 153901.

[40] P. S. Kuo, J. Bravo-Abad, and G. S. Solomon, "Second-harmonic generation using-quasi-phasematching in a GaAs whispering-gallery-mode microcavity," *Nature Commun.*, vol. 5, no. 1, pp. 1–7, 2014.

[41] T. J. Kippenberg, H. Rokhsari, T. Carmon, A. Scherer, and K. J. Vahala, "Analysis of radiation-pressure induced mechanical oscillation of an optical microcavity," *Phys. Rev. Lett.*, vol. 95, no. 3, 2005, Art. no. 033901.

[42] A. Schliesser, P. Del'Haye, N. Nooshi, K. J. Vahala, and T. J. Kippenberg, "Radiation pressure cooling of a micromechanical oscillator using dynamical backaction," *Phys. Rev. Lett.*, vol. 97, no. 24, 2006, Art. no. 243905.

[43] T. J. Kippenberg and K. J. Vahala, "Cavity opto-mechanics," *Opt. Exp.*, vol. 15, no. 25, pp. 17172–17205, 2007.

[44] T. J. Kippenberg and K. J. Vahala, "Cavity optomechanics: Back-action at the mesoscale" *Science*, vol. 321, no. 5893, pp. 1172–1176, 2008.

[45] A. Schliesser and T. J. Kippenberg, "Cavity optomechanics with whispering-gallery mode optical micro-resonators," *Adv. At., Mol., Opt. Phys.*, vol. 58, pp. 207–323, 2010.

[46] S. Weis *et al.*, "Optomechanically induced transparency," *Science*, vol. 330, no. 6010, pp. 1520–1523, 2010.

[47] M. Aspelmeyer, T. J. Kippenberg, and F. Marquardt, "Cavity optomechanics," *Rev. Modern Phys.*, vol. 86, no. 4, 2014, Art. no. 1391.

[48] C. Cao *et al.*, "Tunable high-order sideband spectra generation using a photonic molecule optomechanical system," *Sci. Rep.*, vol. 6, no. 1, pp. 1–8, 2016.

[49] Y.-P. Gao, Z.-X. Wang, X.-F. Liu, T.-J. Wang, and C. Wang, "Optomechanically induced mode transition and spectrum enhancement in a microresonator system," *Annalen der Physik*, vol. 531, no. 7, 2019, Art. no. 1800419.

[50] A. M. Armani, R. P. Kulkarni, S. E. Fraser, R. C. Flagan, and K. J. Vahala, "Label-free, single-molecule detection with optical microcavities," *Science*, vol. 317, no. 5839, pp. 783–787, 2007.

[51] F. Vollmer and S. Arnold, "Whispering-gallery-mode biosensing: Label-free detection down to single molecules," *Nature Methods*, vol. 5, no. 7, pp. 591–596, 2008.

[52] A. Schliesser, G. Anetsberger, R. Rivière, O. Arcizet, and T. J. Kippenberg, "High-sensitivity monitoring of micromechanical vibration using optical whispering gallery mode resonators," *New J. Phys.*, vol. 10, no. 9, 2008, Art. no. 095015.

[53] T. Lu *et al.*, "High sensitivity nanoparticle detection using optical microcavities," *Proc. Nat. Acad. Sci.*, vol. 108, no. 15, pp. 5976–5979, 2011.

[54] M. R. Foreman, J. D. Swaim, and F. Vollmer, "Whispering gallery mode sensors," *Adv. Opt. Photon.*, vol. 7, no. 2, pp. 168–240, 2015.

[55] Y.-P. Gao *et al.*, "Effective mass sensing using optomechanically induced transparency in microresonator system," *IEEE Photon. J.*, vol. 9, no. 1, Feb. 2017, Art. no. 6800411.

[56] T. Reynolds *et al.*, "Fluorescent and lasing whispering gallery mode microresonators for sensing applications," *Laser Photon. Rev.*, vol. 11, no. 2, 2017, Art. no. 1600265.

[57] Y. Zhi, X.-C. Yu, Q. Gong, L. Yang, and Y.-F. Xiao, "Single nanoparticle detection using optical microcavities," *Adv. Mater.*, vol. 29, no. 12, 2017, Art. no. 1604920.

[58] W. Chen, Ş. K. Özdemir, G. Zhao, J. Wiersig, and L. Yang, "Exceptional points enhance sensing in an optical microcavity," *Nature*, vol. 548, no. 7666, pp. 192–196, 2017.

[59] I. S. Grudinin, H. Lee, O. Painter, and K. J. Vahala, "Phonon laser action in a tunable two-level system," *Phys. Rev. Lett.*, vol. 104, no. 8, 2010, Art. no. 083901.

[60] J. Zhang *et al.*, "A phonon laser operating at an exceptional point," *Nature Photon.*, vol. 12, no. 8, pp. 479–484, 2018.

[61] F. Vollmer, S. Arnold, and D. Keng, "Single virus detection from the reactive shift of a whispering-gallery mode," *Proc. Nat. Acad. Sci.*, vol. 105, no. 52, pp. 20701–20704, 2008.

[62] S. Arnold, D. Keng, S. I. Shopova, S. Holler, W. Zurawsky, and F. Vollmer, "Whispering gallery mode carousel-a photonic mechanism for enhanced nanoparticle detection in biosensing," *Opt. Exp.*, vol. 17, no. 8, pp. 6230–6238, 2009.

[63] S. I. Shopova, R. Rajmangal, S. Holler, and S. Arnold, "Plasmonic enhancement of a whispering-gallery-mode biosensor for single nanoparticle detection," *Appl. Phys. Lett.*, vol. 98, no. 24, 2011, Art. no. 243104.

[64] V. R. Dantham, S. Holler, V. Kolchenko, Z. Wan, and S. Arnold, "Taking whispering gallery-mode single virus detection and sizing to the limit," *Appl. Phys. Lett.*, vol. 101, no. 4, 2012, Art. no. 043704.

[65] F. Vollmer and L. Yang, "Review label-free detection with high-Q microcavities: A review of biosensing mechanisms for integrated devices," *Nanophotonics*, vol. 1, no. 3-4, pp. 267–291, 2012.

[66] N. Toropov, G. Cabello, M. P. Serrano, R. R. Gutha, M. Rafti, and F. Vollmer, "Review of biosensing with whispering-gallery mode lasers," *Light: Sci. Appl.*, vol. 10, no. 1, pp. 1–19, 2021.

[67] S. E. Harris, J. E. Field, and A. Imamoğlu, "Nonlinear optical processes using electromagnetically induced transparency," *Phys. Rev. Lett.*, vol. 64, no. 10, 1990, Art. no. 1107.

[68] S. E. Harris, "Electromagnetically induced transparency," *Phys. Today*, vol. 50, no. 7, pp. 36–42, 1997.

[69] A. Lezama, S. Barreiro, and A. M. Akulshin, "Electromagnetically induced absorption," *Phys. Rev. A*, vol. 59, no. 6, 1999, Art. no. 4732.

[70] K.-J. Boller, A. Imamoğlu, and S. E. Harris, "Observation of electromagnetically induced transparency," *Phys. Rev. Lett.*, vol. 66, no. 20, 1991, Art. no. 2593.

[71] A. M. Akulshin, S. Barreiro, and A. Lezama, "Electromagnetically induced absorption and transparency due to resonant two-field excitation of quasidegenerate levels in Rb vapor," *Phys. Rev. A*, vol. 57, no. 4, 1998, Art. no. 2996.

[72] M. Fleischhauer, A. Imamoglu, and J. P. Marangos, "Electromagnetically induced transparency: Optics in coherent media," *Rev. Modern Phys.*, vol. 77, no. 2, pp. 633–673, 2005.

[73] R. Röhlsberger, H.-C. Wille, K. Schlage, and B. Sahoo, "Electromagnetically induced transparency with resonant nuclei in a cavity," *Nature*, vol. 482, no. 7384, pp. 199–203, 2012.

[74] G. S. Agarwal and S. Huang, "Electromagnetically induced transparency in mechanical effects of light," *Phys. Rev. A*, vol. 81, no. 4, 2010, Art. no. 041803.

[75] H. Lü, C. Wang, L. Yang, and H. Jing, "Optomechanically induced transparency at exceptional points," *Phys. Rev. Appl.*, vol. 10, no. 1, 2018, Art. no. 014006.

[76] H. Li, V. A. Sautenkov, Y. V. Rostovtsev, G. R. Welch, P. R. Hemmer, and M. O. Scully, "Electromagnetically induced transparency controlled by a microwave field," *Phys. Rev. A*, vol. 80, no. 2, 2009, Art. no. 023820.

[77] R. Taubert, M. Hentschel, J. Kästel, and H. Giessen, "Classical analog of electromagnetically induced absorption in plasmonics," *Nano Lett.*, vol. 12, no. 3, pp. 1367–1371, 2012.

[78] X. Yang, M. Yu, D.-L. Kwong, and C. W. Wong, "All-optical analog to electromagnetically induced transparency in multiple coupled photonic crystal cavities," *Phys. Rev. Lett.*, vol. 102, no. 17, 2009, Art. no. 173902.

[79] C. Zheng *et al.*, "Controllable optical analog to electromagnetically induced transparency in coupled high-Q microtoroid cavities," *Opt. Exp.*, vol. 20, no. 16, pp. 18319–18325, 2012.

[80] G. Li, X. Jiang, S. Hua, Y. Qin, and M. Xiao, "Optomechanically tuned electromagnetically induced transparency-like effect in coupled optical microcavities," *Appl. Phys. Lett.*, vol. 109, no. 26, 2016, Art. no. 261106.

[81] Y.-C. Liu, B.-B. Li, and Y.-F. Xiao, "Electromagnetically induced transparency in optical microcavities," *Nanophotonics*, vol. 6, no. 5, pp. 789–811, 2017.

[82] J. K. Poon, L. Zhu, G. A. DeRose, and A. Yariv, "Transmission and group delay of microring coupled-resonator optical waveguides," *Opt. Lett.*, vol. 31, no. 4, pp. 456–458, 2006.

[83] Q. Xu, S. Sandhu, M. L. Povinelli, J. Shakya, S. Fan, and M. Lipson, "Experimental realization of an on-chip all-optical analogue to electromagnetically induced transparency," *Phys. Rev. Lett.*, vol. 96, no. 12, 2006, Art. no. 123901.

[84] F. Xia, L. Sekaric, and Y. Vlasov, "Ultracompact optical buffers on a silicon chip," *Nature Photon.*, vol. 1, no. 1, pp. 65–71, 2007.

[85] B. Peng, Ş. K. Özdemir, W. Chen, F. Nori, and L. Yang, "What is and what is not electromagnetically induced transparency in whispering-gallery microcavities," *Nature Commun.*, vol. 5, no. 1, pp. 1–9, 2014.

[86] S. Zhu, L. Shi, S. Yuan, R. Ma, X. Zhang, and X. Fan, "All-optical controllable electromagnetically induced transparency in coupled silica microbottle cavities," *Nanophotonics*, vol. 7, no. 10, pp. 1669–1677, 2018.

[87] A. Naweed, G. Farca, S. I. Shopova, and A. T. Rosenberger, "Induced transparency and absorption in coupled whispering-gallery microresonators," *Phys. Rev. A*, vol. 71, no. 4, 2005, Art. no. 043804.

[88] C. Wang *et al.*, "Electromagnetically induced transparency at a chiral exceptional point," *Nature Phys.*, vol. 16, no. 3, pp. 334–340, 2020.

[89] A. H. Safavi-Naeini *et al.*, "Electromagnetically induced transparency and slow light with optomechanics," *Nature*, vol. 472, no. 7341, pp. 69–73, 2011.

[90] G. Morigi, J. Eschner, and C. H. Keitel, "Ground state laser cooling using electromagnetically induced transparency," *Phys. Rev. Lett.*, vol. 85, no. 21, 2000, Art. no. 4458.

[91] Y. Xu, R. K. Lee, and A. Yariv, "Propagation and second-harmonic generation of electromagnetic waves in a coupled-resonator optical waveguide," *JOSA B*, vol. 17, no. 3, pp. 387–400, 2000.

[92] J. J. Longdell, E. Fraval, M. J. Sellars, and N. B. Manson, "Stopped light with storage times greater than one second using electromagnetically induced transparency in a solid," *Phys. Rev. Lett.*, vol. 95, no. 6, 2005, Art. no. 063601.

[93] H. A. Haus and W. Huang, "Coupled-mode theory," *Proc. IEEE*, vol. 79, no. 10, pp. 1505–1518, Oct. 1991.

[94] M. J. Humphrey, E. Dale, A. T. Rosenberger, and D. K. Bandy, "Calculation of optimal fiber radius and whispering-gallery mode spectra for a fiber-coupled microsphere," *Optics. Commun.*, vol. 271, no. 1, pp. 124–131, 2007.

[95] C.-L. Zou *et al.*, "Taper-microsphere coupling with numerical calculation of coupled-mode theory," *JOSA B*, vol. 25, no. 11, pp. 1895–1898, 2008.

[96] C. W. Gardiner and M. J. Collett, "Input and output in damped quantum systems: Quantum stochastic differential equations and the master equation," *Phys. Rev. A*, vol. 31, no. 6, 1985, Art. no. 3761.

[97] M. D. Stenner, D. J. Gauthier, and M. A. Neifeld, "The speed of information in a 'fast-light' optical medium," *Nature*, vol. 425, no. 6959, pp. 695–698, 2003.

[98] Z. Yang, "Physical mechanism and information velocity of fast light: A time-domain analysis," *Phys. Rev. A*, vol. 87, no. 2, 2013, Art. no. 023801.

[99] J. Ghosh, R. Ghosh, F. Goldfarb, J.-L. Le Gouët, and F. Bretenaker, "Analysis of electromagnetically induced transparency and slow light in a hot vapor of atoms undergoing collisions," *Phys. Rev. A*, vol. 80, no. 2, 2009, Art. no. 023817.

[100] C. Jiang, H. Liu, Y. Cui, X. Li, G. Chen, and B. Chen, "Electromagnetically induced transparency and slow light in two-mode optomechanics," *Opt. Exp.*, vol. 21, no. 10, pp. 12165–12173, 2013.

[101] T. Wang, Y.-Q. Hu, C.-G. Du, and G.-L. Long, "Multiple EIT and EIA in optical microresonators," *Opt. Exp.*, vol. 27, no. 5, pp. 7344–7353, 2019.